Application of time–resolved–pulsed–EPR spectroscopy to study photoinduced electron transfer reactions. –Porphyrin/quinone system–

Masamoto Iwaizumi*, Kouta Yamamoto, Yasunori Ohba, and Seigo Yamauchi

Institute for Chemical Reaction Science, Tohoku University, Katahira, Sendai, 980 (Japan)

ABSTRACT

Characteristic features of the time–resolved fourier transform EPR (FT–EPR) and electron spin echo FT–EPR (ESE–FT–EPR) spectroscopies for studies of photochemical reaction kinetics are summarized in comparison with the cw–time–resolved EPR (CW–TREPR) spectroscopy. The former two methods were applied to study the photoinduced electron transfer reaction between zinc tetraphenylporphyrin (ZnTPP) and benzoquinone (BQ) in 2–butanol. It is shown that deuterium substitution of the compounds and an application of the ESE–FT–EPR method are effective to observe the broad EPR spectrum of the ZnTPP cation which is missed in measurements by FT–EPR. The kinetic data obtained for the deuterated and undeuterated compounds are compared.

A. INTRODUCTION

The time resolved EPR(TREPR) spectroscopy has been used as a powerful technique for investigations of photochemical reaction kinetics. The advantage of the EPR spectroscopy for reaction kinetic studies comes from the following features. (1) EPR observes only paramagnetic species so that spectra are relatively simple. (2) Identification of species is, in most cases, simple even when plural paramagnetic species are present, and their behaviors can be followed. (3) In many cases, structural information can be obtained from spectra. (4) Spin polarization produced in reaction processes provides valuable information not only on reaction kinetics but also on spin dynamics.

The cw method in TREPR has been widely used for reaction kinetic studies because of the instrumental simplicity [1–3]. However, nowadays rapidly developing pulsed EPR spectroscopy has more advantages than the cw method and is becoming a more powerful technique. In this article, we shortly summarize characteristics of a newly developing fourier transform EPR (FT–EPR) spectroscopy, and present application to a study of photoinduced electron transfer reactions between zinc tetraphenylporphyrin (ZnTPP) and benzoquinone (BQ). FT–EPR is powerful for invesitgations of this field, but one problem in

0010-8545/94/$26.00
SSDI 0010-8545 (94) 02003-2

this method is to miss broad EPR signals. In this article, we present an attempt to use deuterium substituted compounds and the method of electron spin echo FT-EPR (ESE-FT-EPR) to observe broad EPR spectra. The effects of the deuterium substitution on the reaction kinetics and spin dynamics are presented.

B. CW-TREPR, FT-EPR AND ESE-FT-EPR SPECTROSCOPIES

CW-TREPR spectra are obtained by measuring time dependence of EPR signals following initiation of the reaction by laser light at a given magnetic field and a spectrum at a given time is observed by sweeping the magnetic field [1]. In this method, signal intensities are mainly determined by dynamic spin polarization (CIDEP) effect produced in the chemical reaction processes, so that observation of EPR spectra is, in most cases, limited to the period in which the spin is polarized.

In FT-EPR, the magnetization of paramagnetic species is flipped down to the xy plane (perpendicular to the magnetic field direction) by a 90° microwave pulse and the measured free induction decay (FID) signal is fourier transformed to a frequency domain FT-EPR spectrum [1,4]. For the sake of direct observation of magnetization, the FT-EPR spectroscopy has higher sensitivity than CW-TREPR. It enables observation of paramagnetic species not only in the polarized spin state but also in the thermal spin population.

The FT-EPR spectroscopy has also higher spectral and time resolution than CW-TREPR. In CW-TREPR, when inverse of the time delay between radical formation and signal detection becomes comparable to or exceeds the intrinsic linewidth, the recorded EPR lines show appreciable broadening by the uncertainty principle. In FT-EPR, the signal is detected over a longer time period of free induction decay, and hence such linewidth broadening does not occur. In FT-EPR, the resonant cavity of low Q value is used to obtain a wide bandwidth of the microwave pulse. The use of the low Q cavity also results in high time resolution; the Q value of 100 gives time resolution of 10 ns, about 10 times higher than that in the CW-TREPR. It may be notable that in FT-EPR measurement time can be appreciably shorten compared to the cw method because of the multichannel properties of the pulsed method. One problem met in FT-EPR is to miss broad EPR signals, because their components in FID decay during the spectrometer dead time after the microwave pulse.

It is known that shape of the Hahn's echo is composed of two FID's attached back to back. Therefore, FT of the one half of the spin echo signal gives the spectrum corresponding to the ordinary FT-EPR spectrum. This method, which can be called ESE-FT-EPR, is expected to be effective for observation of broad EPR signals, because loss of the FID signal during the instrumental dead time can be avoided in measurements of Hahn's echo signals.

C. EXPERIMENTAL PROCEDURE

TPP having deuterium substituted phenyl groups (TPP-d_{20}) were synthesized from toluene-d_8 according to the literature [5]. Deuterated benzoquinone (BQ-d_4) was obtained from phenol-d_6. 2-Butanol solutions of ZnTPP and BQ or of their deuterated compounds were degassed on a vacuum line for spectral measurements. Typical concentrations of ZnTPP and BQ were 5 x 10^{-5} M and 3 x 10^{-3} M, respectively.

FT-EPR and ESE-FT-EPR spectra were measured by a home made pulsed EPR spectrometer [6,7]. For spectral measurements, ZnTPP was excited at the S_1 region by a Lambda Physik LPX 100i excimer laser (XeCl, 308 nm) pumped Lambda Physik LPD 3000 dye laser. Measurements of FT-EPR and ESE-FT-EPR spectra were performed at 23°C.

D. RESULTS AND DISCUSSION

The FT-EPR spectrum obtained for the ZnTPP and BQ system at the delay time of 200 ns is shown in Fig.1a. The observed signals showing emission (E) and absorption (A) are assigned to BQ^- and the E/A pattern of the spectrum is attributed to the CIDEP effect arising mainly from the ST_0 radical pair mechanism (RPM). The signal with the first derivative like line shape comes from the dispersion component of the spin correlated radical pair between $ZnTPP^+$ and BQ^- [4]. In CW-TREPR, the three species, BQ^-, $ZnTPP^+$ and their radical pair, were observed [3,4], but in FT-EPR $ZnTPP^+$ was not recorded because of the large linewidth due to the unresolved hyperfine lines. As Fig.1b shows, the missing $ZnTPP^+$ signal became observable when ZnTPP-d_{20} and BQ-d_4 were used. Time evolution of the FT-EPR spectra for the ZnTPP-BQ system is shown in Fig.2. Compared to the cw-method, the FT-EPR spectra were observed for a surprisingly long period (10 ns ~ 200 μs) after photoirradiation.

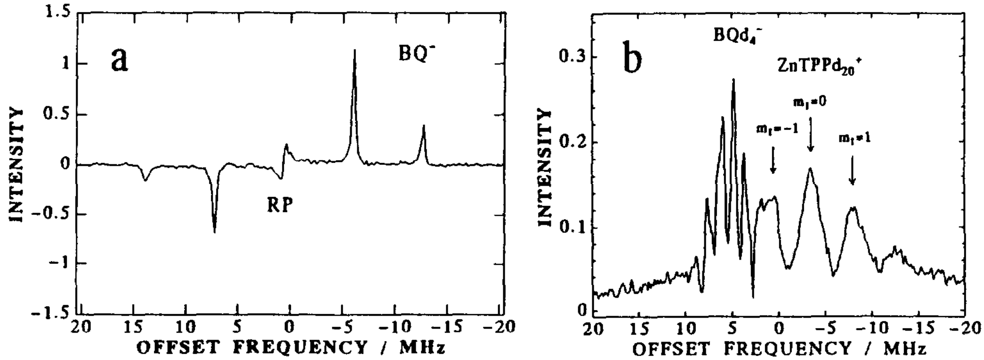

Fig.1. FT-EPR spectra for (a) the ZnTPP/BQ system observed at 200 ns after the laser pulse and (b) for the ZnTPP-d_{20}/BQ-d_4 system at 40 ns after the laser pulse. The spectrum in (a) was processed by the LP-SVD method [8,9] and the spectrum in (b) is expressed as a power spectrum.

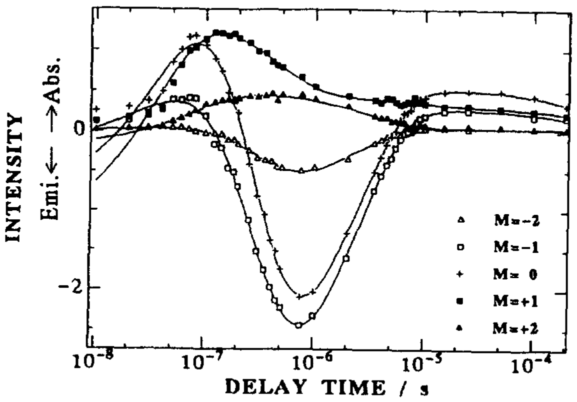

Fig.2. Time evolution of FT-EPR spectra of BQ⁻ in the ZnTPP/BQ system. The solid lines are the ones calculated by using the constants in Table 1.

As Fig. 2 shows, at the early stage after photoirradiation the spectra show an absorptive type pattern, then the E/A pattern appears, and finally all hyperfine lines become absorptive type followed by the decrease of the signal amplitudes. These changes with time are explained by the following reaction scheme [4].

$$\mathrm{ZnTPP} \xrightarrow{h\nu} {}^1\mathrm{ZnTPP}^* \xrightarrow{\mathrm{isc}} {}^3\mathrm{ZnTPP}^*$$

$${}^3\mathrm{ZnTPP}^* + \mathrm{Q} \xrightarrow{k_{et}} [\mathrm{ZnTPP}^+ ... \mathrm{Q}^-] \xrightarrow{k_{ce}} \mathrm{ZnTPP}^+ + \mathrm{Q}^-$$

$$\mathrm{ZnTPP}^+ + \mathrm{Q}^- \xrightarrow{k_b} \mathrm{ZnTPP} + \mathrm{Q}$$

The radicals produced from the polarized triplet spin state show the TM CIDEP effect exhibited by enhancement absorption component. The electron transfer reaction from the T_0 triplet component gives ST_0–RPM polarization with an E/A pattern. The TM effect gives equal contribution to pair of hyperfine lines with nuclear spin of M and -M, and the RPM effect gives difference in signal amplitudes of M and -M lines. Growth of the signal amplitude difference, therefore, reflects formation of BQ⁻ so that it can be used to evaluate the rate constant for the radical formation. On the other hand, decrease of the TM component reflects spin lattice relaxation process T_{1T} in the triplet state of ZnTPP. The signal amplitude decreases in the later part of time evolution reflect the spin–lattice relaxation process T_{1R} in the generated radical BQ⁻ and back electron transfer reaction. Especially at the delay times after the 10^{-5} s from the laser pulse excitation, the spin polarization is mostly lost and the observed absorptive type signals come from the radical in the thermal spin equilibrium. Hence the EPR intensity changes in this region directly reflect changes of the radical concentration.

The time evolutions in Fig. 2 were analyzed by the least square fitting according to the above processes. In the analyses, back electron transfer reaction was not taken into account because the effect is minor except for the time evolution at time delays longer than 10^{-5} s. The pseudo first order rate constant of the radical formation and spin-lattice relaxation times obtained for the both undeuterated and deuterated compound systems are listed in Table 1. The time evolutions calculated by the constants in Table 1 are compared with experimental ones in Fig. 2 and they are well fit with the experimental ones.

TABLE 1 Rate constant and spin lattice relaxation times

	ZnTPP-d_{20}/BQ-d_4	ZnTPP/BQ
rate constant,k_{et}/$M^{-1}s^{-1}$	2.7×10^9	2.7×10^9
spin relaxation time, T_{1T}/ns	27	22
spin relaxation time,T_{1R}/µs	2.8	2.6

The time dependence of signal intensities at the region after delay time of 10^{-5} s are plotted in logarithm scale for the deuterated compound system in Fig. 3, which shows that the plots for the cation and the anion change in parallel with time. This indicates that ratio of the signal intensities between the both cation and anion is constant with time; they must be returning to the initials by back electron transfer reaction with the second order rate process.

As Table 1 shows, the rate constant of the electron transfer reaction does not

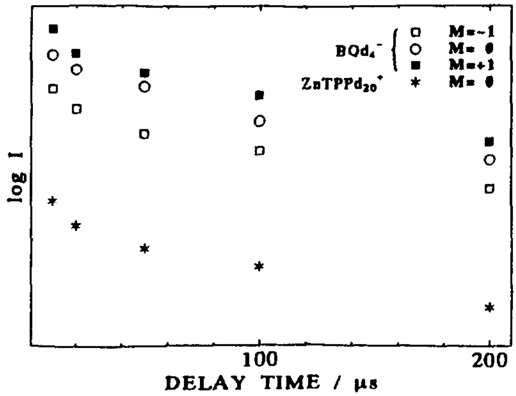

Fig.3. Log plots of the signal intensities after delay time of 10 µs for the ZnTPP-d_{20}/BQ-d_4 system.

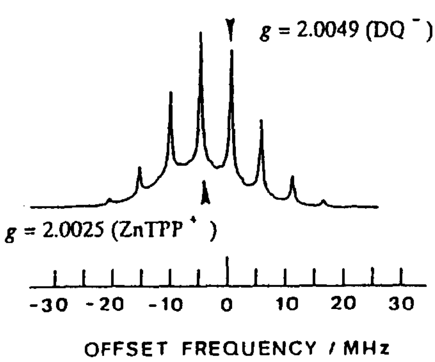

Fig. 4. ESE-FT-EPR spectrum for the ZnTPP/DQ system at 1 µs after the laser pulse.

change with deuterium substitution of ZnTPP and BQ. However, the spin-lattice relaxation times, T_{1T} and T_{1R}, become longer by the deuterium substitution. This indicates that the hyperfine interaction plays some roles on the spin relaxation processes, and the deuterium substitution, which gives smaller hyperfine couplings, results in decreasing contribution of the hyperfine interaction to the spin lattice relaxation processes.

It is shown above that deuterium substitution are effective for observation of broad EPR spectra. The ESE-FT-EPR spectroscopy is another useful method for the purpose [7]. An example of ESE-FT-EPR applied to the ZnTPP and duroquinone (DQ) system is shown in Fig. 5 where the both $ZnTPP^+$ and DQ^- signals are clearly recorded. Time evolution of the signals of DQ^- was compared with that obtained by the ordinary FT-EPR spectra. The both time evolutions are well agreed each other [7]. This means that the method of ESE-FT-EPR will become a powerful technique for investigations of reaction kinetics, especially for systems containing EPR signals with large linewidths which may be missed by FT-EPR.

In the present work, the behaviors of the radical pair have not been discussed, but they contain important and interesting problems on reaction kinetics. Including such problems, further studies on solvent effects and substituents effects on the reaction processes are in progress.

E. ACKNOWLEDGEMENT

This work was partially supported by Grant-in-Aid for Scientific Research on Priority Area "Molecular Magnetism" (Area No.228/No.05226205), 02554015 and 03554014 from the Ministry of Education, Science and Culture, Japan.

F. REFERENCES

1 L. Kevan, M.K. Bowman (eds.), Modern Pulsed and Continuous-Wave Electron Spin Resonance, Wiley, New York, 1990.
2 H.van Willigen, M. Vuolle, K.P. Dinse, J. Phys. Chem., 93 (1989) 2441.
3 S. Yamauchi, T. Ueda, M. Satoh, K. Akiyama, S. Tero-Kubota, Y. Ikegami and M. Iwaizumi, J. Photochem. Photobiol. A:Chem., 65 (1922) 177.
4 H.van Willigen, P.R. Levstein, and M.H. Ebersole, Chem. Rev., 93 (1993) 173, and references therein.
5 L.A. Dust and E.W. Gill, J. Chem. Soc. C, (1970) 1631.
6 Y. Ohba, R. Satoh, T. Kikuchi, S. Yamauchi and M. Iwaizumi, J. Magn. Reson., A 103 (1993) 282.
7 Y. Ohba, N. Okabe, R. Satoh, K. Yamamoto, S. Yamauchi and M. Iwaizumi, Appl. Magn. Reson., in press.
8 H. Barkhuijsen, R.de Beer, W.M.M.J. Bovée, and D.van Ormondt, J. Magn. Reson., 61 (1985) 465.
9 M. Uike, T. Uchiyama and H. Minamitani, J. Magn. Reson., 99 (1992) 363.